Manuscript submitted to
AIMS' Journals
Volume **X**, Number **0X**, XX **200X**

Website: http://AIMsciences.org
pp. **X–XX**

CONTINUATION AND BIFURCATIONS OF BREATHERS IN A FINITE DISCRETE NLS EQUATION

Panayotis Panayotaros

Depto. Matemáticas y Mecánica
I.I.M.A.S.-U.N.A.M.
Apdo. Postal 20–726, 01000 México D.F., México

Abstract. We present results on the continuation of breathers in the discrete cubic nonlinear Schrödinger equation in a finite one-dimensional lattice with Dirichlet boundary conditions. In the limit of small inter-site coupling the equation has a finite number of breather solutions and as we increase the coupling we see numerically that all breather branches undergo either fold or pitchfork bifurcations. We also see branches that persist for arbitrarily large coupling and converge to the linear normal modes of the system. The stability of the breathers that persist generally changes as the coupling is varied, although there are at least two branches that preserve their linear and nonlinear stability properties throughout the continuation.

1. **Introduction.** In the present work we study the continuation and bifurcations of breather solutions of the discrete cubic nonlinear Schrödinger equation (DNLS) in a finite one dimensional lattice with open boundary conditions. The equation is a simple model for many systems where we see a combination of nonlinear and spatial inhomogeneity effects, e.g. in optical waveguide array systems [6], Bose-Einstein condensates (BEC) in a periodic magnetic field [16], and in electron transport in solid state systems, or biomolecules [15]. Depending on the system size, it is of interest to study both few-site and larger (or infinite) lattices, e.g. in some optics, and BEC applications of the DNLS a few-site model seems more appropriate, while in molecular or solid state systems one may consider an infinite lattice model. From the theoretical point of view, the subtle differences in the long time dynamics of finite and infinite lattice systems, e.g. in coherent structures that may exist in the finite lattice but decay slowly in the infinite system (see [5] for likely examples), also call for studies of both types of systems.

A breather solution of the DNLS is a solution if the form $u_n = e^{-i\omega t} A_n$, where n is the lattice index, ω is the temporal frequency, and A_n is the time-independent breather amplitude. In an infinite lattice, where we also require that A_n decay at infinity, breathers can be viewed as the simplest spatially localized solutions. In a finite DNLS, localization can also be an important feature of some breather solutions (i.e. when A_n decays rapidly away from certain sites), but we are primarily interested in the temporal periodicity of breathers, and the fact that breathers are relative equilibria. We use these properties to see that (most) breathers are fixed

2000 *Mathematics Subject Classification.* Primary: 37J20, 35Q55; Secondary: 37J45, 37M20, 37L60.

Key words and phrases. Discrete NLS equations, breathers, bifurcations.

.

points in a suitable reduced phase space. The reduction construction is elementary and generalizes the change to action-angle coordinates used in the integrable 2-site lattice. It also appears only applicable to the finite one-dimensional DNLS with Dirichlet boundary conditions. The reduction is global, in the sense that it is defined in the whole of phase space minus some codimension-one (or smaller) sets, that may however include breathers. Thus breathers can be thought of as the simplest invariant sets of the DNLS system, and a starting point for a study of the global dynamics of the DNLS. The reduction construction seems most useful in small lattices, where we use it to find bifurcations of breathers in $2-$, and $3-$site lattices (also considered in [8], [12]). The types of bifurcations we see there are representative of the bifurcations we see in larger systems.

In studying larger lattices we use the fact that in the finite DNLS system with Dirichlet boundary conditions and weak inter-site coupling we have a finite number of breather solutions. These breathers can be continued from trivial breather solutions of the system with zero inter-site coupling (the "anticontinuous limit" system), moreover many of their stability properties can be deduced using ideas from studies of the infinite lattice ([18], [20]). A further property of the system is that all breathers are real. We remark that there are related finite lattice systems with analogous solutions at the weak coupling regime. However, the number of such solutions can be infinite; this is the case for the finite one dimensional DNLS with periodic boundary conditions (see [10]), higher dimensional finite DNLS systems (see [21], [19]), and discrete sine-Gordon systems (see [4]). Thus the finite one-dimensional DNLS system with Dirichlet boundary conditions is special and allows us, at least in principle, to consider the more global question of continuing numerically all breathers as the inter-site coupling increases.

The results we present mainly concern the continuation of breathers that are symmetric or antisymmetric under spatial reflection. We see evidence that as we increase the inter-site coupling the majority of breather branches undergo fold bifurcations where two branches collide and both solutions disappear. Some examples of folds were earlier seen in [2]. There is also evidence for pitchfork bifurcations where three branches originating from small inter-site coupling breathers collide, and one can be continued past the bifurcation point. Although the collisions studied systematically here involve branches of breathers with the same symmetry type (symmetric or antisymmetric) there is also evidence for collisions of symmetric and non-symmetric branches, e.g. we see a possible double fold involving two symmetric and two non-symmetric branches. In all cases we observe that the bifurcations are subcritical, i.e. the number of branches decreases as we increase $|\delta|$. This does not seem to be the case in the periodic lattice (see [10]).

For an $N-$site lattice we also see N branches that are continued to arbitrary large inter-site coupling. These breathers are symmetric or antisymmetric and in the limit of infinite coupling they are seen to converge to the normal modes of the linear DNLS, i.e. the eigenvectors of the discrete Laplacian. The possibility of such a continuation was discussed earlier in [2]. We also study the stability of these branches. We see that there are always two branches of nonlinearly (orbitaly) stable breathers that may be heuristically characterized as "spatially localized" and " spatially delocalized" respectively.

In the computations we report we increase the inter-site coupling keeping the power (l_2 norm of the solutions) constant. Also, as we try different lattices we consider a power that is roughly proportional to the number of sites, i.e. we keep the "power per site" fixed. These choices are made to simplify the numerics, moreover we show that the results apply to the problem of varying both coupling and power.

The related problem of the continuation of breathers of the DNLS in the infinite lattice was studied in [1]. The number of anti-continuous limit breathers is infinite in that case, and a comprehensive numerical study of all breather branches is not possible. Nevertheless, the types of bifurcations seen in both cases appear to be the same. Similarities and differences between the finite and infinite problems are discussed further in Section 4.

The paper is organized as follows. In Section 2 we describe the reduced phase space for the finite DNLS. In Section 3 we state general results on breathers, especially on weak inter-site coupling breathers. We also use the reduced phase space to study bifurcations of breathers in small lattices. In Section 4 we present numerical results on the continuation and bifurcation of symmetric and antisymmetric breathers in larger lattices.

2. **Hamiltonian structure and reduction.** We consider the discrete NLS equation

$$\dot{u}_n = i\delta(\Delta u)_n - 2i|u_n|^2 u_n, \tag{1}$$

where n ranges over the finite set $\iota_N = \{1, \ldots, N\}$ of lattice sites, and the discrete Laplacian Δu is defined by

$$(\Delta u)_n = u_{n+1} + u_{n-1} - 2u_n, \quad n = 2, \ldots, N-1 \tag{2}$$

$$(\Delta u)_1 = u_2 - 2u_1, \quad (\Delta u)_N = u_{N-1} - 2u_N. \tag{3}$$

The particular form of $(\Delta u)_1$, $(\Delta u)_N$ corresponds to *Dirichlet* boundary conditions. The site coupling constant δ is real. System (1) is equivalent to Hamilton's equation

$$\dot{u}_n = -i\frac{\partial H}{\partial u_n^*}, \quad n \in \iota_N, \quad \text{with} \tag{4}$$

$$H = \delta\left(\sum_{n=1}^{N-1} |u_{n+1} - u_n|^2 + |u_1|^2 + |u_1|^2\right) + \sum_{n=1}^{N} |u_n|^4. \tag{5}$$

The conserved quantities of system (1) are the Hamiltonian H, and the "power"

$$P = \sum_{n\in\iota_N} |u_n|^2. \tag{6}$$

The conservation of P comes from the invariance of H under the map $u_n \mapsto e^{i\theta}u_n$, $n \in \iota_N$, where θ is an arbitrary real number that is independent of n.

We can use the conservation of P, and a composition of elementary canonical transformations to explicitly reduce the dimension of the phase space of (4) by 2. First, using real and imaginary parts $q_n = \mathrm{Re}u_n$, $p_n = \mathrm{Im}u_n$, $n \in \iota_N$, and letting $h = \frac{1}{2}H$, system (4) is written as

$$\dot{q}_n = \frac{\partial h}{\partial p_n}, \quad \dot{p}_n = -\frac{\partial h}{\partial q_n}, \quad n \in \iota_N. \tag{7}$$

Introducing polar coordinates $u_n = \sqrt{J_n}e^{i\phi_n}$, Hamilton's equations take the form

$$\dot{\phi}_n = -\frac{\partial h}{\partial J_n}, \quad \dot{J}_n = \frac{\partial h}{\partial \theta_n}, \quad n \in \iota_N, \quad \text{with} \tag{8}$$

$$h = \frac{1}{2}\delta\left(\sum_{n=1}^{N-1}[J_{n+1} + J_n - 2\sqrt{J_{n+1}J_n}\cos(\phi_{n+1} - \phi_n)] + J_1 + J_N\right) + \frac{1}{2}\sum_{n=1}^{N} J_n^2. \tag{9}$$

Furthermore, define the angles θ_n and actions I_n by

$$\theta_n = \phi_{n+1} - \phi_n, \quad n = 1, \ldots, N-1, \quad \theta_N = \sum_{n=1}^{N} \phi_n \tag{10}$$

$$J_1 = I_1 + I_N, \quad J_n = I_n - I_{n-1} + I_N, \quad n = 2, \ldots, N-1, \quad J_N = I_N - I_{N-1}. \tag{11}$$

The above define implicitly a canonical transformation and Hamilton's equation (8) become

$$\dot{\theta}_n = -\frac{\partial h}{\partial I_n}, \quad \dot{I}_n = \frac{\partial h}{\partial \theta_n}, \quad n \in \iota_N, \tag{12}$$

with h the Hamiltonian in terms of the θ_n, J_n. We observe that h is independent of θ_N. Then I_N is a conserved quantity, and by (11),

$$I_N = N^{-1} \sum_{n=1}^{N} J_n = N^{-1} P, \tag{13}$$

i.e. we recover the conservation of the power.

Setting $I_N = c$, with c an arbitrary positive constant, the *reduced system* is

$$\dot{\theta}_n = -\frac{\partial h}{\partial I_n}, \quad \dot{I}_n = \frac{\partial h}{\partial \theta_n}, \quad n \in \{1, \ldots, N-1\}, \tag{14}$$

where

$$h = -\delta \sum_{n=1}^{N-1} \sqrt{J_{n+1} J_n} \cos \theta_n + \frac{1}{2} \sum_{n=1}^{N} J_n^2, \tag{15}$$

with

$$J_1 = I_1 + c, \quad J_n = I_n - I_{n-1} + c, \quad n = 2, \ldots, N-1, \quad J_N = c - I_{N-1}. \tag{16}$$

Let $\mathtt{Y}_j \subset \mathbf{R}^{2N}$ be the set of points $[q_1, \ldots, p_N] \in \mathbf{R}^{2N}$ satisfying $q_j = p_j = 0$. Let $\mathtt{Y} = \cup_{j=1}^{N} \mathtt{Y}_j$. Also consider the set $\mathtt{S}$ of $[I_1, \ldots, I_N] \in \mathbf{R}^N$ satisfying $J_k > 0$, $k = 1, \ldots, N$, where the J_k are as in (11). Let $\mathbf{T}^k$ denote the $k-$dimensional torus. Then, (10), (11) define a smooth symplectic transformation from $\mathbf{R}^{2N} \setminus \mathtt{Y}$ to $\mathtt{S} \times \mathbf{T}^N$, Also, let $\mathtt{S}_c^{N-1}$ be the the set of $[I_1, \ldots, I_{N-1}] \in \mathbf{R}^{N-1}$ that satisfy $J_k > 0$, $k = 1, \ldots, N$, where the J_k are as in (16). The reduced system is defined in the reduced phase space $\mathtt{S}_c^{N-1} \times \mathbf{T}^{N-1}$.

Remark 1. Reduction via use of the θ_n, I_n variables is applicable to the DNLS with site-dependent δ (as in models with "disorder"), and to the DNLS equations with time-dependent parametric forcing, such as diffraction management (see [9]).

3. **Relative equilibria and breathers.** A *breather* solution of (1) is a periodic solution of (1) of the form $u_n = e^{-i\omega t} A_n$, with ω real, and $A = [A_1, \ldots, A_N] \in \mathbf{C}^N \setminus \{0\}$ independent of t. By (1), A, ω satisfy

$$-\omega A_n = \delta (\Delta A)_n - 2|A_n|^2 A_n, \quad n \in \iota_N. \tag{17}$$

Note that if A satisfies (17) so does $e^{i\phi} A$, for arbitrary real ϕ independent of n. A *real* breather is a breather of the form with $e^{i\phi} \tilde{A}$, where $\tilde{A} \in \mathbf{R}^N$, and ϕ is an arbitrary real independent of n. A *nowhere-zero breather* is a breather with $A_n \neq 0$, $\forall n \in \iota_N$. The set of *nodes* $\mathtt{N}$ of a breather A consist of the $n \in \iota_N$ satisfying $A_n = 0$.

Proposition 1. *Let $\delta \neq 0$. Then all breathers are real.*

Proof. By the breather Ansatz $u_n = e^{-i\omega t} A_n$, the phases of the u_n have the same angular velocity, and the moduli are constant. Then, by the definition of the variables θ_n, I_n above, each nowhere-zero solution of (1) can be identified with a fixed point of the reduced DNLS (14). The correspondence in onto, and 2 to 1. By (15), fixed points of (14) must satisfy

$$\frac{\partial h}{\partial \theta_n} = \delta \sqrt{J_{n+1} J_n} \sin \theta_n = 0, \quad n \in \{1, \dots, N-1\}, \tag{18}$$

thus $\theta_n = 0$, or π, $\forall n \in \{1, \dots, N-1\}$ (since the J_n are positive). Thus nowhere-zero breathers are real.

Consider a breather whose set of nodes $\mathtt{N}$ is nonempty. In the case where $\mathtt{N}$ contains at least two consecutive nodes, there exists a $j \in \mathtt{N}$ such that either $j-1$, or $j+1$ is not on $\mathtt{N}$. By $\delta \neq 0$ we see that the $j-$th equation of (17) can not be satisfied. Thus the nearest neighbors of any $j \in \mathtt{N}$ belong to $\iota_N \setminus \mathtt{N}$. We consider two cases. In the case where $\mathtt{N}$ is $\{1\}$, or $\{N\}$, or $\{1, N\}$, we can use polar coordinates and similarly define variables θ_n, I_n for the sites in $\iota_N \setminus \mathtt{N}$, i.e. the breather corresponds to a nowhere-zero breather in a smaller lattice. The reality of breathers follows then as in the case of nowhere-zero breathers. In the case where $\mathtt{N} \neq \{1\}$, $\{N\}$, or $\{1, N\}$, there exists a $j \in \mathtt{N}$, such that if $j \pm 1 \in \mathtt{N}$ then $j \pm 1 \in \iota_N \setminus \mathtt{N}$. Let j_L be the nearest site to the left of j that is either in $\mathtt{N}$, in which case let $B_L(j) = \{j_L + 1, \dots, j-1\}$, or in $\{1\}$, in which case let $B_L(j) = \{1, \dots, j-1\}$. Also, let j_R be the nearest site to the right of j that is either in $\mathtt{N}$, in which case let $B_R(j) = \{j+1, \dots, j_R - 1\}$, or in $\{N\}$, in which case let $B_R(j) = \{j+1, \dots, N\}$. Arguing as in the previous case we use polar coordinates, the variables θ_n, I_n, and the argument for nowhere-zero breathers for the sites of B_L to see that the breather, restricted to B_L, has the form $A_n = e^{i\phi_L} \tilde{A}_n$, with $\tilde{A}_n \in \mathbf{R}$, $\forall n \in B_L$, and ϕ_L an arbitrary real that is independent of $n \in B_L$. Similarly we see that the breather, restricted to B_R, is real up to an arbitrary real phase ϕ_R. By $\delta \neq 0$ we see that the $j-$th equation of (17) implies then that, $\phi_L = \pm \phi_R$ (modulo 2π). Applying the argument to other sites $j \in \mathtt{N}$ with $j \pm 1 \in \iota_N \setminus \mathtt{N}$, we see that the breather is real. □

The reality statement also holds for the infinite one-dimensional lattice, see [24]. The argument here is different. The impossibility of neighboring nodes was also noted in [14].

Remark 2. The frequency ω of a nowhere-zero breather corresponding to a fixed point of the reduced system can be recovered in the following way. Let $\tilde{\theta} = [\tilde{\theta}_1, \dots, \tilde{\theta}_{N-1}] \in \mathbf{T}^{N-1}$, $\tilde{I} = [\tilde{I}_1, \dots, \tilde{I}_{N-1}] \in \mathtt{S}_c^{N-1}$ be a fixed point of the reduced system. Let $\lambda = \frac{\partial h}{\partial I_N}$, evaluated at $\theta_j = \tilde{\theta}_j$, $I_j = \tilde{I}_j$, $j = 1, \dots, N-1$, $I_N = c$. By (12) we then have $\theta_N(t) = \lambda t + \theta_N(0)$, while for $j = 1, \dots, N-1$ we have $\theta_j(t) = \tilde{\theta}_j$, $\forall t$. Inverting the linear system (10) by the Jordan algorithm we see that $\phi_j = N^{-1}\theta_N + \sigma_j$, $j = 1, \dots, N$, where the σ_j are linear combinations of $\theta_1, \dots, \theta_{N-1}$. It then follows that $\omega = N^{-1}\lambda$. (By Proposition 1 the σ_j are integer multiples of π; this can be also verified directly by inverting (10).) In the case of breathers with nodes we use the same procedure for a set of sites between nodes. The assumption that we have a breather for the N site lattice, and the observation above that in the sites between nodes we have a nowhere-zero breather of a smaller lattice imply that the ω found for different sublattices between nodes must coincide.

To look for breather solutions we start with small $|\delta|$ breathers. These are continued from solutions of (17) with $\delta = 0$. In particular, given any $U \subset \iota_N$, (17) with

$\delta = 0$ has solutions of the form

$$A_n = e^{i\phi_n}\sqrt{\frac{\omega}{2}}, \quad \text{for} \quad n \in U; \quad A_n = 0, \quad \text{for} \quad n \in U^c, \tag{19}$$

with $\omega > 0$, and arbitrary $\phi_n \in \mathbf{R}$.

The basic continuation result states that all real breathers of the $\delta = 0$ system can be continued to real breathers of the $\delta \neq 0$ system.

Proposition 2. *Let $\omega > 0$ and consider $U \subset \iota_N$. Let $A(0) \in \mathbf{C}^N$ be a solution of the form (19) of the $\delta = 0$ breather equation (17) that satisfies $\phi_n = 0$, or π, $\forall n \in U$. Then there exists $\tilde{\delta} > 0$ such that for any $\delta \in (-\tilde{\delta}, \tilde{\delta})$ equation (17) has a unique real solution $A(\delta) \in \mathbf{R}^N$ that satisfies $A(\delta) \to A(0)$ as $\delta \to 0$. The dependence of $A(\delta)$ on δ is real analytic in $(-\tilde{\delta}, \tilde{\delta})$. Moreover, any continuous one-parameter family $A(\delta)$, $\delta \in (-\tilde{\delta}, \tilde{\delta})$, of breathers that satisfies $A(\delta) \to A(0)$ as $\delta \to 0$, is a one-parameter family of real breathers.*

An analogous proposition was originally shown for an infinite lattice in [20]. The arguments used in the infinite case apply with minor modifications to the present case and the proof is omitted. In the finite case the proof can be also simplified using the real breather continuation result of [17], and Proposition 1.

In the numerical study below we are mainly interested in the fixed power continuation problem, where we have similar statement. In this variant of the problem we fix $C > 0$ and look for $A \in \mathbf{C}^N \setminus \{0\}$, $\omega \in \mathbf{R}$ that satisfy

$$-\omega A_n = \delta(\Delta A)_n - 2|A_n|^2 A_n, \quad n \in \iota_N, \quad \sum_{n \in \iota_N} |A_n|^2 = C. \tag{20}$$

Given any $U \subset \iota_N$, the breather equation (20) with $\delta = 0$ has solutions of the form

$$A_n = e^{i\phi_n}\sqrt{\frac{\omega}{2}}, \quad \text{for} \quad n \in U; \quad A_n = 0, \quad \text{for} \quad n \in U^c; \quad \omega = \frac{2C}{|U|} \tag{21}$$

where the $\phi_n \in \mathbf{R}$ are arbitrary, and $|U|$ is the cardinality of U.

Proposition 3. *Fix $C > 0$ and consider $U \subset \iota_N$. Let $A(0) \in \mathbf{C}^N$, $\omega(0)$ be a solution of the form (21) of the $\delta = 0$ breather equation (20) that satisfies $\phi_n = 0$, or π, $\forall n \in U$. Then there exists $\tilde{\delta}$ such that for any $\delta \in (-\tilde{\delta}, \tilde{\delta})$ equation (20) has a unique solution $A(\delta) \in \mathbf{R}^N$, $\omega(\delta) \in \mathbf{R}$ that satisfies $A(\delta) \to A(0)$ as $\delta \to 0$. The dependence of $A(\delta)$ on δ is real analytic in $(-\tilde{\delta}, \tilde{\delta})$.*

Proof. By Proposition 1 it is enough to look for real solutions of the breather equation. Let $C > 0$. Let $X = \mathbf{R}^{N+1}$, and for $[A_1, \ldots, A_N, \omega] \in \mathbf{R}^{N+1}$, $\delta \in \mathbf{R}$ define the function $F : X \times \mathbf{R} \to X$ by

$$F_n = \omega A_n + \delta(\Delta A)_n - 2A_n^3, \quad n = 1, \ldots, N; \quad F_{N+1} = \frac{1}{2}\left(\sum_{n=1}^{N} A_n^2 - C\right). \tag{22}$$

By (20) real breathers are solutions of $F = 0$. Let x_0 satisfy $F(x_0, 0) = 0$, i.e. x_0 is of the form (21) with $\phi_n = 0$, π, $\forall n \in U$. We check that the matrix $[D_1 F](x_0, 0)$ is nonsingular. By the real analyticity of F in its domain, and the implicit function theorem we then have a $\tilde{\delta} > 0$ and a unique real analytic family of $x(\delta) \in X$, $|\delta| < \tilde{\delta}$, satisfying $F(x(\delta), \delta) = 0$, and $x(\delta) \to x_0$ as $\delta \to 0$. $\square$

Corollary 1. *There exists δ_0 such that all solutions of the $\delta \neq 0$ breather equation (17) with $|\delta| < \delta_0$ are obtained by continuation from the real breather solutions of the $\delta = 0$ breather equation.*

Proof. By Proposition 1 for $\delta \neq 0$ it is sufficient to examine solutions of $F = 0$. By Proposition 3 and the fact that at $\delta = 0$ we have a finite set of real breathers, we have the existence of branches of breathers continued from the $\delta = 0$ real breathers for all $|\delta| < \tilde{\delta}_0$, where $\tilde{\delta}_0$ is the minimum of the $\tilde{\delta}$ for each $\delta = 0$ real breather of Proposition 3. Thus for $|\delta| < \tilde{\delta}_0$ we have the breather solutions obtained by continuing the $\delta = 0$ real breathers. To show the statement for some $\delta_0 > 0$, $\delta_0 \leq \tilde{\delta}_0$, assume that on the contrary there exists a sequence of $\{\epsilon_n\}_{m=1}^{\infty} \to 0$, $\epsilon_m \leq \tilde{\delta}_0$, $\forall m \geq 1$, such that the breather equation with $\delta = \epsilon_m$ has at least one solution $x_m = [A_1(m), \ldots, A_N(m), \omega(m)]$ that stays away from the set of the $\delta = 0$ real breathers, Multiplying the $j-$th equation of (17) by A_j, summing over the j, and using $\sum_{j=1}^{N} A_j^2 = C$, there exists some $\Omega > 0$ for which $\omega(m) \leq \Omega$, $\forall m \geq 1$. Then the sequence of the pairs (ϵ_m, x_m) has a convergent subsequence (ϵ_μ, x_μ), satisfying $F(x_\mu, \epsilon_\mu) = 0$, $\forall \mu$, and $\epsilon_\mu \to 0$, $x_\mu \to \chi$ for some $\chi \in \mathbf{R}^{N+1}$. By the continuity of F, χ is a $\delta = 0$ real breather, a contradiction. $\square$

A breather obtained by continuing a $\delta = 0$ breather with $|U| = k$ is referred to as a $k-$*peak breather*.

By the above, for small enough $|\delta|$ we know all breather solutions and they can be obtained by continuing the $\delta = 0$ real breathers. For a lattice of N sites, each $\delta = 0$ real breather and its unique continuation (for small $|\delta|$) can be labeled by an array $[s(1), \ldots, s(N)]$, where $s(j) = 0$, for $j \in \mathtt{N}$, and $s(j) = +1$, -1, for $\phi_j = 0$, π respectively. For a lattice of N sites we thus have $3^N - 1$ distinct $\delta = 0$ real breathers. Furthermore, for $|\delta|$ sufficiently small the reduced phase space has at most $\frac{(3^N-1)}{2}$ fixed points, i.e. we may have breathers with nodes. Fixed points of the reduced phase space can be labeled by the arrays used for the $\delta = 0$ breathers, with arrays related by a global sign flip identified.

Remark 3. In the finite lattice system we expect that we can also continue higher dimensional invariant tori of the $\delta = 0$ equations (in addition to the $2-$tori of [3]). The reduced phase space construction shows that breathers are the simplest invariant sets of the DNLS system in a global sense. A drawback of the reduction is that it introduces artificial singularities at ∂S_c, where polar coordinates are not well defined. For instance breathers with nodes belong to ∂S_c and can not be studied using the reduced phase space construction.

Remark 4. In the case of the finite lattice with periodic boundary condition and $N > 2$, we do not have a similar reduction. For instance, the definition (10) does not lead to a similar cyclic variable reduction, while the possible $\theta_n = \phi_{n+1} - \phi_n$, $n = 1, \ldots, N-1$, $\theta_N = \phi_1 - \phi_N$ is singular. At the same time we can see that in the periodic problem we have $N-$peak breather solutions that are not real; their existence can be shown by the argument used in [21] to show the existence of discrete vortices in two dimensions.

Some of the general features of the continuation of breathers can be obtained by examining the simplest cases of lattices of two, three, and four sites where it is possible to visualize bifurcations. We consider the cases of two, and three sites where the visualization is simpler. In what follows we set $P = C$, or $I_N = c = \frac{C}{N}$, i.e. compare (13), (20).

Example 1: Two sites.

In this case the system is integrable. Let $u_n = J_n e^{i\phi_n}$, and define

$$\theta_1 = \phi_1 - \phi_2, \quad \theta_2 = \phi_2 + \phi_1, \quad I_1 = \frac{1}{2}(J_1 - J_2), \quad I_2 = \frac{1}{2}(J_2 + J_1), \tag{23}$$

as in (11), (10). Letting $\theta = \theta_1$, $I = I_1$, $I_2 = c$, the Hamiltonian reduces to

$$h = -I^2 - \delta\sqrt{c^2 - I^2}\cos\theta \tag{24}$$

and is defined in the phase space $|I| < c$, $\theta \in S^1$. (S^1 is the interval $[0, 2\pi]$ with 0, 2π identified). For $|\delta|$ small we expect four breather solutions. These are shown in Figure 1, where we plot the contours of the Hamiltonian h at $\delta = -2$, $c = 3$. At $\theta = \pi$, $I = 0$ we see the $[1, -1]$ fixed point (corresponding to a 2−peak breather). At $\theta = 0$, $I = 0$ we see the $[1, 1]$ fixed point (2−peaks), and the fixed points $[1, 0]$, and $[0, 1]$ (1−peak). As δ decreases further, the 1−peak fixed points move closer to $I = 0$, i.e. the difference in amplitudes at each peak decreases, while the 2−peak fixed points remain at $I = 0$. At about $\delta = -5.5$ the contour plot suggests that the three $\theta = 0$ fixed points collide at $I = 0$. Afterwards there is only one fixed point, at $I = 0$. This is indicated in the contours of h at $\delta = -6$, $c = 3$, see Figure 2. We thus have evidence for a pitchfork bifurcation. For $\delta > 0$ we have the same contours, shifted by π.

Note that the two site system has been analyzed along similar lines by [8] (it is also known as the dimer system, see [11]). The bifurcations of breathers were seen in [12] who also considered the addition of a potential that breaks the symmetry between the two sites. By Remark 1 the reduction is still valid for this and more general perturbations.

Example 2: Three sites.

Let $u_n = J_n e^{i\phi_n}$, and define the variables θ_n, I_n by

$$\theta_1 = \phi_1 - \phi_2, \quad \theta_2 = \phi_3 - \phi_2, \quad \theta_3 = \phi_1 + \phi_2 + \phi_3 \tag{25}$$

$$J_1 = I_1 + I_3, \quad J_2 = I_2 - I_1 + I_3, \quad J_3 = I_3 - I_2 \tag{26}$$

as in (11), (10). Letting $I_3 = c$, the Hamiltonian reduces to

$$\begin{aligned} h &= \frac{1}{2}[(I_1 + c)^2 + (I_2 - I_1 + c)^2 + (c - I_2)^2] \\ &\quad -\delta[\sqrt{(I_1 + c)(I_2 - I_1 + c)}\cos\theta_1 + \sqrt{(I_2 - I_1 + c)(c - I_2)}\cos\theta_2], \end{aligned} \tag{27}$$

with $(\theta_1, \theta_2) \in S^1 \times S^1$, $(I_1, I_2) \in \mathtt{S}^2_c$, where $\mathtt{S}^2_c$ is the set of $(I_1, I_2) \in \mathbf{R}^2$ satisfying $I_1 > -c$, $I_2 < c$, $I_2 - I_1 > c$. These restrictions follow from $J_k > 0$, $k = 1, 2, 3$. $\mathtt{S}^2_c$ is a triangle with edges at $(-c, c)$, $(-c, -2c,)$, $(2c, c)$ and each side corresponds to the vanishing of one of the three J_k.

To find nowhere-zero breathers we fix the vector (θ_1, θ_2) to one of the values $(0, 0)$, $(0, \pi)$, $(\pi, 0)$, (π, π) and look for critical points of $h(\theta_1, \theta_2)$ for $(I_1, I_2) \in \mathtt{S}^2_c$.

For $(\theta_1, \theta_2) = (0, 0)$, and $\delta = -2.5$, $c = 3$, we see the 1−peak fixed points $[1, 0, 0]$, $[0, 1, 0]$, $[0, 0, 1]$, the 2−peak fixed points $[1, 1, 0]$, $[1, 0, 1]$, $[0, 1, 1]$, and the 3−peak fixed point $[1, 1, 1]$. Note that for $|\delta|$ small, fixed points $[s(1), \ldots, s(N)]$ with $s(j) = 0$ for some j are near the sides of the triangle and are difficult to detect by contour plots of $h(\theta_1, \theta_2)$. For instance, in Figure 3, we are showing a piece of the triangle $\mathtt{S}^2_c$, $c = 3$, for $\delta = -1.4$. Near $(-3, 3)$ we see the $[0, 1, 0]$ fixed point and further to the right we have the fixed point $[1, 1, 0]$. Both are near the segment $(-3, 3)$, $(6, 3)$, the side corresponding to $J_3 = 0$. As we decrease δ further, the fixed points remain away from the sides of the triangle and we see pairs of fixed points that merge and disappear. First we see that $[1, 1, 1]$, and $[1, 0, 1]$ approach each other, merge, and disappear at $\delta \approx -1.8$, in what appears to be a fold bifurcation. At $\delta \approx -5.7$ we see the merger and disappearance of $[1,0,0]$, and $[1,1,0]$. By symmetry this also happens to the pair $[0,0,1]$, and $[0,1,1]$. In Figure 4 we magnify a piece of the triangle to locate the continuations of $[0,1,1]$ (top), and $[0,0,1]$ (bottom) at $\delta = -5.6$. Note that they have both moved significantly, e.g. $[0,0,1]$ goes to the corner $(-3,-6)$ as $\delta \to 0$. In Figure 5 we see the same region at $\delta = -5.8$; apparently the two breathers have merged and disappeared. After about $\delta = -5.8$ only the breather $[0,1,0]$ survives. Decreasing δ further suggest that this breather exists for δ arbitrarily small.

For $(\theta_1, \theta_2) = (\pi, 0)$ we see the merger and disappearance of the fixed points $[1,-1,-1]$, and $[1,-1,0]$, while for $(\theta_1,\theta_2) = (0,\pi)$ we see the same for the fixed points $[1,1,-1]$, and $[0,1,-1]$. For $(\theta_1,\theta_2) = (\pi,\pi)$ we see the fixed $[1,-1,1]$ that appears to persist for δ arbitrarily small.

The above 12 fixed points of the correspond to 24 nowhere-zero breathers. The missing breathers are $[1,0,-1]$, and $[-1,0,1]$, this suggests that these breathers have a node at the middle site, $\forall \delta \neq 0$.

The above qualitative analysis is corroborated by solving (20) directly, as in the next section. In particular, we verify the three basic collisions between *(i)* $[1,1,1]$, $[1,0,1]$ at $\delta = -1.790$, *(ii)* $[1,-1,-1]$, $[1,-1,0]$ at $\delta = -2.335$, and *(ii)* $[1,1,0]$, $[1,0,0]$ at $\delta = -5.760$. The corresponding relative angles are as above. (All other colliding branches are obtained by the above three via reflections with respect to the middle site or via the inversion $A \to -A$.) We also see evidence that $[0,+,0]$, $[-1,1,-1]$, $[-1,0,1]$, and their respective inversions can be continued to $|\delta|$ arbitrarily negative and verify that breathers $[-,0,+]$, $[+,0,-]$ that were not seen in the above picture have a node, $\forall \delta < 0$.

By (27) we see that for $\delta > 0$ we obtain a similar bifurcation scenario, e.g. the contour plots for (π,π), $\delta > 0$ coincide with the ones for $(0,0)$, $-\delta < 0$.

Remark 5. A similar correspondence between positive and negative δ nowhere-zero breathers holds for arbitrary N. This follows from (15), (16). By the arguments in the proof of Proposition 1 the correspondence holds also for breathers with nodes.

In [13] a similar but slightly different system of three equations is derived to approximate breathers in an NLS equation with a three well potential. The breathers considered there have a similar identification with strings of $+1$, -1, 0, and despite the difference in the intermediate steps, the bifurcation scenario observed (summarized in Figure 3 of [13]) seems the same as the one we see here. An explanation of these similarities is outside the scope of the present work, we do point out however that the comparison of the theory with direct simulation of the breather for the PDE in [13] supports the idea that the bifurcation scenarios found for DNLS lattices can be relevant to or have analogues with bifurcations in the NLS equations they approximate, independently of the question of how good these approximations are.

4. Bifurcations in larger chains.

In this section we consider the numerical continuation of breathers in δ in larger lattices by studying the solutions of the equation $F = 0$ of (22), i.e. (20). This approach allows us to continue all breathers obtained for $|\delta|$ sufficiently small, without being restricted to nowhere-zero breathers. The numerical strategy here is to continue each breather by increasing $|\delta|$ in suitably small steps, until some criterion tells us to stop the continuation. The general idea, to be justified a-posteriori, is that monitoring where branches stop is sufficient for detecting and characterizing all possible bifurcations. By a breather *branch* (starting at A_0) we here denote a differentiable one-parameter family of solutions $[A(\delta), \omega(\delta)]$ of (20) with $\delta \in (-\delta_0, 0]$, $\delta_0 \in \mathbf{R}^+$, that also satisfies $A(0) = A_0$.

In what follows, the power P will be held fixed to a constant C as we vary δ. Furthermore, we let C be proportional to N, i.e. we fix the "power per site". For $|\delta|$ sufficiently small, this scaling keeps ω bounded away from zero, i.e. by (20), and $P = cN$ we have $\omega \geq 2c > 0$ at $\delta = 0$ (see also Remark 7 below).

Due to the large number of breathers we have so far restricted our study to symmetric and antisymmetric breathers. Given a breather $A = [A_1, \ldots, A_N] \in \mathbf{R}^N$, define its reflection $B \in \mathbf{R}^N$ by $B = [B_1, \ldots, B_N] = [A_N, \ldots, A_1]$. A breather is *symmetric* if $B = A$, and *antisymmetric* if $B = -A$. Note that F preserves symmetry and antisymmetry and we can restrict the equation $F = 0$ to the respective subspaces. In the results below we instead consider the full system and verify numerically that branches that start at symmetric (antisymmetric) $\delta = 0$ breathers consist of symmetric (antisymmetric) breathers. We also consider $\delta < 0$, i.e. decrease δ. By Remark 5 the continuation of nowhere-zero breathers should give the same results for both signs of δ, up to a permutation of the branches. The numerical results suggest that for $\delta \neq 0$ the symmetric breathes have no nodes.

In Figures 6, 7 we plot δ vs. ω for all branches of symmetric breathers obtained for $N = 7$, 13 respectively. The graph suggests that there are many branches that collide and disappear, as in $N = 3$. There is also a number of branches that are continued up to the largest $|\delta|$ shown. In the cases of apparent branch collisions, we verify that they correspond to pairs of distinct branches that terminate at some δ, where all components of the solution $x = [A, \omega]$ of $F = 0$ coincide. Both breather branches consist of symmetric breathers. As suggested by Figure 6, for $N = 7$ there also 4 branches that may be continued to $|\delta|$ arbitrarily large. For $N = 13$ we have 7 branches with that property, see Figure 7. In these examples, a branch of symmetric breathers either collides with another branch in a fold bifurcation, or can be continued to δ arbitrarily negative.

Continuation of antisymmetric breathers for $N = 7$ yields a similar scenario, with folds involving pairs of branches of antisymmetric branches, and a number of branches that can be continued to δ arbitrarily negative. In Figure 8 we plot δ vs. ω for all branches of antisymmetric breathers obtained for $N = 13$. In addition to folds involving pairs of antisymmetric breathers, and branches that can be continued to $|\delta|$ arbitrarily large (without intersecting other branches), we also see evidence for pitchfork bifurcations involving antisymmetric breathers. We see three examples of pitchforks. One of them is indicated in Figure 9, where we plot the A_4 component of breathers that are continued from the $\delta = 0$ breathers $[-1, 1, -1, -1, 1, -1, 0, \ldots]$, $[-1, 1, -1, 0, 1, -1, 0, \ldots]$, $[-1, 1, 0, -1, 1, -1, 0, \ldots]$. The numerical continuation of two of the branches (corresponding to the second and third breathers) is terminated at the apparent bifurcation point, at approximately $\delta = -3.5$, while a third branch is continued to $|\delta|$ arbitrarily large.

In the numerical continuation of symmetric and antisymmetric breathers we see that in a lattice of N sites the number of breathers that can be continued for $|\delta|$ arbitrarily large is N. Moreover as we increase $|\delta|$ these N breathers converge to the N solutions v of $\Delta v = \lambda v$ (normalized to $\sum_{j=1}^{N} v_j^2 = C$), while the slopes $-\frac{\omega}{\delta}$ converge to the eigenvalues λ. The convergence of breathers that persist for large $|\delta|$ to eigenvectors of Δ (the linear normal modes) should follow from the fact that the term $\delta(\Delta A)_n$ dominates the nonlinearity A_n^3 as $|\delta|$ increases, i.e. since

$\sup_{n\in\iota_N}|A_n|^2 \leq C$. Examples for $N = 13$ are shown in Figure 10. There we compare breathers for the branches starting at the $\delta = 0$ symmetric breathers $[0, 0, 0, 0, 0, 0, 1, \ldots]$ (top), $[-1, 1, -1, 1, 0, -1, 1, \ldots]$ (bottom) to the respective linear normal modes to which they converge. Convergence is slower for the branch of the first breather, which is more localized and whose $\sup_{n\in\iota_N}|A_n|^2$ is larger. Specifically, in the top picture the comparison is with a breather at $\delta = -75.0$, while in the picture we use a breather obtained for $\delta = -7.5$.

In summary, all examples examined so far suggest that the possible bifurcations of symmetric and antisymmetric breathers are folds and pitchforks. Also, in all fold and pitchfork bifurcations we see that the number of branches decreases only in the direction of increasing $|\delta|$, i.e. all bifurcations are subcritical.

Also, in all symmetric and antisymmetric cases above we observe numerically that DF has a simple eigenvalue that approaches zero as we approach the bifurcation point δ_0. By standard arguments this implies a one dimensional bifurcation equation with one parameter, i.e. an equation of the form $f(x, \epsilon) = 0$, with x, $\epsilon = \delta - \delta_0$. The possibility of determining f from the numerics will be analyzed in further work.

Note that the study of symmetric and antisymmetric breathers does not give a the whole picture since there is evidence of bifurcations involving symmetric or antisymmetric breathers (some pitchforks of this type are reported in [2]). An interesting example is seen at $N = 5$, where we have the collision and disappearance of the symmetric branches $[-1, -1, -1, \ldots]$, $[-1, 0, -1, \ldots]$ with the non-symmetric branches $[-1, 0, -1, -1, -1]$, $[-1, -1, -1, 0, -1]$ at approximately $\delta = -0.705$, i.e. a double fold bifurcation. In this example the nullspace of DF at the bifurcation is two dimensional.

Remark 6. To solve $F = 0$ we used the minpack implementation of Powell's hybrid Newton's method (see [7], [22]). The criterion for stopping the continuation is the failure of convergence for the Newton's method. This is a crude criterion but it has been efficient in the examples described in the figures, e.g. it has allowed us to continue past pitchforks with only a few cases of branch switching. More refined strategies near the suspected bifurcation point are currently under consideration.

Remark 7. Setting $a_n = \frac{A_n}{\sqrt{C}}$, $\tilde{\omega} = \frac{\omega}{C}$, equation (20) becomes

$$-\tilde{\omega}a_n = \tilde{\delta}(\Delta a)_n - 2|a_n|^2 a_n, \quad n \in \iota_N, \quad \sum_{n\in\iota_N}|a_n|^2 = 1, \tag{28}$$

with $\tilde{\delta} = \frac{\delta}{C}$. Thus the breather equation has only one parameter and by varying δ with C fixed we are studying the general case. Keeping C proportional to N has a numerical advantage however. In the results obtained this way we see that the first bifurcations occur for a range of δ that does depend on N. In (28) such bifurcations would correspond to a range of $\tilde{\delta}$ of size $\sim N^{-1}$. Solving (28) would then require that we vary $\tilde{\delta}$ using smaller steps as we increase N.

Remark 8. Breather bifurcations in the infinite one-dimensional DNLS were studied in [1] using the symplectic map interpretation of the breather equation (with ω fixed, and P undetermined). The bifurcations seen in that work correspond to the fold and pitchfork bifurcations we see here and they also appear to subcritical. We have also examined some of the breather branches seen in $N-$site lattices in larger lattices. We saw cases where the breather branches appear to converge as we increase the size of the larger lattice. There are however cases of bifurcations seen in the $N-$site lattice system that do not persist in a larger lattice. Some of these differences can be explained by the lack of translation symmetry in the finite problem. For instance, for N odd we see that the branches continued from off-center one-peak anticontinuous limit breathers eventually disappear as $|\delta|$ is increased, i.e. only the breather at the center appears to converge to a linear normal mode as $|\delta|$ increases. In the infinite lattice the one-peak breather exists for $-\delta$ arbitrarily large; this follows from the variational interpretation of the breather equation and the absence of a power threshold in one dimension, see [23]. Also in the infinite problem there are no finite l_2 norm normal modes: breathers that persist for arbitrary $|\delta|$ must converge to the trivial solution in the (weaker) l_∞ norm.

We conclude we some remarks on the stability of the breathers seen in this study. These are based on a comparison between the theoretically expected stability properties of small $|\delta|$ breathers, and numerical results on the stability of the continued branches.

To study the (relative) stability of a breather $u = e^{-i\omega t}A$, we write the DNLS in the variables v defined by $u = e^{-i\omega t}v$. In this system the breather is a fixed point. The linearized equation has the form $\dot{v} = J\mathtt{H}$, where $\mathtt{H} = \nabla^2 H_\omega(A)$, the Hessian of $H_\omega = H - \omega P$ at A. For a $k-$peak breather in an $N-$site lattice, and $|\delta|$ sufficiently small we expect the following.

The spectrum of $J\mathtt{H}$ consists of *(i)* a double zero eigenvalue, *(ii)* $2(N-k)$ imaginary eigenvalues (in pairs $\pm i\omega + O(\delta)$), and *(iii)* $2k-2$ eigenvalues that can be either real (in pairs $\pm O(\sqrt{\delta})$), or imaginary (in pairs $\pm iO(\sqrt{\delta})$). Furthermore, the spectrum of $\mathtt{H}$ consists of *(i)* one zero (simple) eigenvalue, *(ii)* $2(N-k)$ negative eigenvalues (of absolute value $O(1)$), *(iii)* $k-1$ positive eigenvalues (of size $O(1)$), and *(iv)* k eigenvalues of size $O(\delta)$ (that can be positive or negative).

The above scenario is an extrapolation of results obtained for an infinite lattice, with ω fixed (see [18], [20]). The results on the parts *(i)*, *(iii)* of the spectrum of $J\mathtt{H}$ should follow from the arguments used in the infinite problem. The eigenvalues of part *(ii)* of $J\mathtt{H}$ are seen numerically in examples and correspond to "remnants" of the continuous spectrum of $J\mathtt{H}$: for a given $k-$peak breather that is found numerically in a lattice with increasing N (and that appears to converge to a breather of the infinite problem), we see that the eigenvalues of part *(ii)* of $J\mathtt{H}$ become denser in two bounded intervals on the imaginary axis that approach the continuous spectrum of $J\mathtt{H}$ in the infinite lattice. (Analogous observations apply to $\mathtt{H}$.)

By the above general picture, linear stability is determined by the eigenvalues of part *(ii)* (see [18], [20] for more information). Also, for $2 \le k \le N-1$, $\mathtt{H}$ has at least two positive, and two negative eigenvalues, therefore the only breathers that can be a local minima or maxima of H_ω restricted to $P = C$ are $1-$peak breathers, and some $N-$peak breathers. We note that local minima and maxima of H_ω restricted to $P = C$ are nonlinearly (orbitaly) stable breathers. On the other hand, trajectories starting near a linearly stable breather that is not a local extremum of H_ω restricted to $P = C$ may stay near the breather orbit for a long time, but it is not clear that they will stay near the breather for all time.

Most nonlinearly stable breathers of the small $|\delta|$ regime disappear as $\delta < 0$ is decreased. As noted in Remark 8, for N odd, the $1-$peak breather whose peak is located at the middle site persists to arbitrary $\delta < 0$, while all other $1-$peak breathers disappear through fold bifurcations. For N even, most $1-$peak breathers disappear through folds. There are also pairs of $1-$peak breather branches that collide with a symmetric multi-peak branch in a pitchfork bifurcation; the symmetric branch then persists for arbitrary $\delta < 0$, as in $N = 2$. Similarly, it appears that only one of the $N-$peak breathers persist for arbitrary $\delta < 0$.

In examining the breathers that persist for arbitrary $\delta < 0$ we see that their linear stability can change as we vary δ. There are many scenarios of change of stability. For example, in Figure 11 we show the real part of all eigenvalues of $J\mathtt{H}$ for the symmetric breather $[-1, 1, -1, 1, 0, -1, 1, \ldots]$. It is indicated that there are intervals of δ where the real part of all eigenvalues vanishes, these are (roughly) $-0.2 < \delta \leq 0$, and $\delta < -3.1$, i.e. for the remaining values of δ we have instability.

Also, for N odd we see two branches, originating in a $1-$peak, and an $N-$peak breather respectively, that remain nonlinearly stable for all $\delta < 0$. For $|\delta|$ small these $1-$peak breathers may be thought of as stable spatially localized states, while $N-$peak breathers may be thought of as stable delocalized (or power equipartition) states. These two branches respectively correspond to unique global maxima and minima of H on $P = C$. This follows from the numerical spectra of the Hessian $\mathtt{H}$, and should explain their persistence to arbitrary $\delta < 0$. For N even, we also have the persistence of two branches connected to $1-$peak, and $N-$peak breathers, with the additional phenomenon of the merging of two distinct global maxima.

Acknowledgements. We would like to thank L. Cisneros, J. Ize, J. Lebowitz, and A. Vanderbauwhede for helpful discussions and comments. This work was partially supported by SEP-Conacyt 50303, and FENOMEC.

REFERENCES

[1] G.L. Alfimov, V.A. Brazhnyi, V.V. Konotop, *On classification of intrinsic localized modes for the discrete nonlinear Schrödinger equation*, Physica D 194 (2004), 127–150.
[2] Yu.V. Bludov, V.V. Konotop, *Surface modes and breathers in finite arrays of nonlinear waveguides*, Phys. Rev. E 76, (207), 046604.
[3] D. Bambusi, D. Vella, *Quasi periodic breathers in Hamiltonian lattices with symmetries*, Discrete Contin. Dyn. Syst. Ser. B 2, (2002), 389–399.
[4] L.A. Cisneros, J. Ize, A.A. Minzoni, *Modulational and numerical solutions for the steady discrete Sine-Gordon equation in two space dimensions*, Physica D, to appear.
[5] L.A. Cisneros, A.A. Minzoni, P. Panayotaros, N.F. Smyth, *Modulation analysis of large scale discrete vortices*, Phys. Rev. E 78 (2008), 036604.
[6] D.N. Christodoulides, F. Lederer, Y. Silberberg, *Discretizing light behavior in linear and nonlinear lattices*, Nature 424 (2003), 817–823.
[7] J.J. Dongarra, C.B. Moler, *Eispack, a package for solving eigenvalue problems*, in Sources and development of mathematical software, W.J. Cowell, ed., Prentice-Hall, New York, 1984.
[8] J.C. Eilbeck, P.S. Lomdahl, A.C. Scott, *The discrete self-trapping equation*, Physica D 16 (1985) 318–338.
[9] H.S. Eisenberg, Y. Silberberg, R. Morandotti, J.S. Aitchison, *Diffraction management*, Phys. Rev. Lett. 85 (2000), 1863.
[10] C.L. Pando, E.J. Doedel, *Bifurcation structures and dominant modes near relative equilibria in the one dimensional discrete nonlinear Schrödinger equation*, Physica D 238 (2009), 687–698.
[11] V.M. Kenkre, D.K. Campbell, *Self-trapping on a dimer: Time-dependent solution of a discrete nonlinear Schrödinger equation*, Phys. Rev. B 34 (1986), 4959–4961.
[12] T. Kapitula, P.G. Kevrekidis, *Bose-Einstein condensates in the presence of a magnetic trap and optical lattice: two-mode approximation*, Nonlinearity 18 (2005), 2491–2512.
[13] T. Kapitula, P.G. Kevrekidis, Z. Chen, *Three is a crowd: Solitary Waves in Photorefractive Media with Three Potential Wells*, SIAM J. Appl. Dyn. Syst. 5 (2007), 598–633.
[14] P.G. Kevrekidis, V.V. Konotop, *Bright compact breathers*, Phys. Rev. E 65 (2002), 066614.
[15] G. Kopidakis, S. Aubry, G.P. Tsironis, *Targeted energy transfer through discrete breathers in nonlinear systems*, Phys. Rev. Lett. 87 (2001), 165501.
[16] R. Livi, R. Franzosi, G. Oppo, *Self-localization of Bose-Einstein condensates in optical lattices via boundary dissipation*, Phys. Rev. Lett. 97 (2006), 060401.

[17] R.S. MacKay, S. Aubry, *Proof of existence of breathers for time-reversible or Hamiltonian networks of weakly coupled oscillators*, Nonlinearity 7 (1994), 1623–1643. Physica D 37, 829-839 (2008)

[18] P. Panayotaros, *Linear stability of real breathers in the discrete NLS*, Phys. Lett. A 373 (2009), 957–963.

[19] P. Panayotaros, D.E. Pelinovsky, *Periodic oscillations of discrete NLS solitons in the presence of diffraction management*, Nonlinearity 21 (2008) 1265–1279.

[20] D.E. Pelinovsky, P.G. Kevrekidis, D.J. Frantzeskakis, *Stability of discrete solitons in nolinear Schrödinger lattices*, Physica D 212 (2005), 1–19.

[21] D.E. Pelinovsky, P.G. Kevrekidis, D.J. Frantzeskakis, *Persistence and stability of discrete vortices in nonlinear Schrödinger lattices*, Physica D 212 (2005) 20–53.

[22] M.J.D. Powell, *A hybrid method for nonlinear equations, in Numerical methods for nonlinear algebraic equations*, P. Rabinowitz, ed., Gordon and Breach, New York, 1970.

[23] M.I. Weinstein, *Excitation thresholds for nonlinear localized modes on lattices*, Nonlinearity 12, (1999) 673-691.

[24] W. Qin, X. Xiao, *Homoclinic orbits and localized solutions in nonlinear Schrödinger lattices*, Nonlinearity 20 (2007), 2305–2317.

Received xxxx 20xx; revised xxxx 20xx.

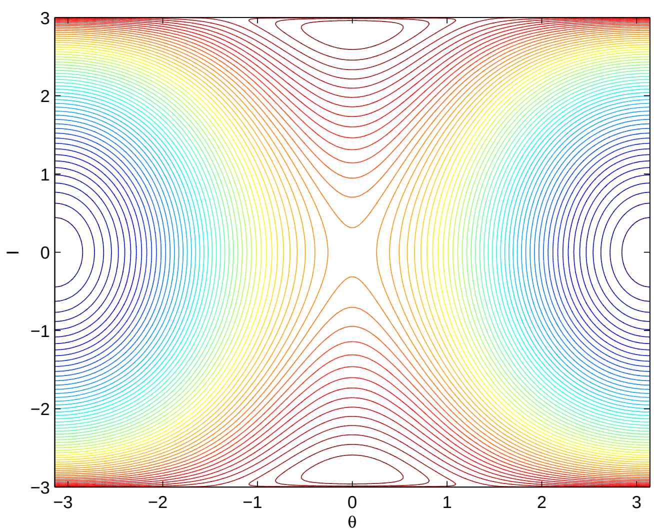

FIGURE 1. **Contours of the Hamiltonian** h **of (24) in the** $(\theta, I)-$**plane.** $c = 3$**,**$\delta = -2$**.**

E-mail address: panos@mym.iimas.unam.mx

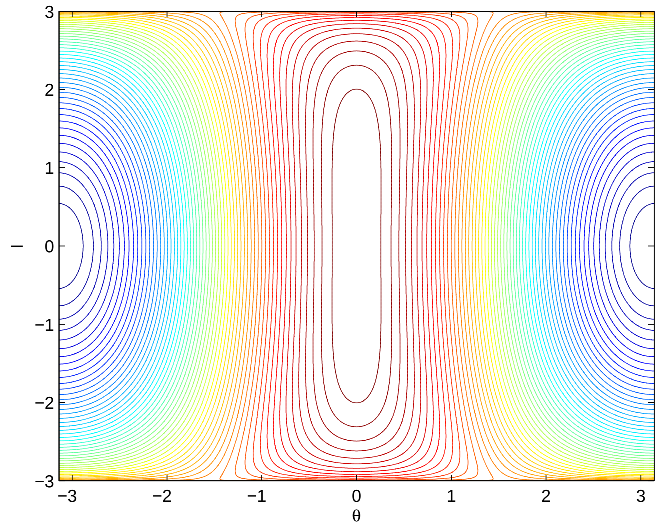

FIGURE 2. Here is the Caption of your figure. **Contours of the Hamiltonian h of (24) in the $(\theta, I)-$plane. $c = 3$, $\delta = -6$.**

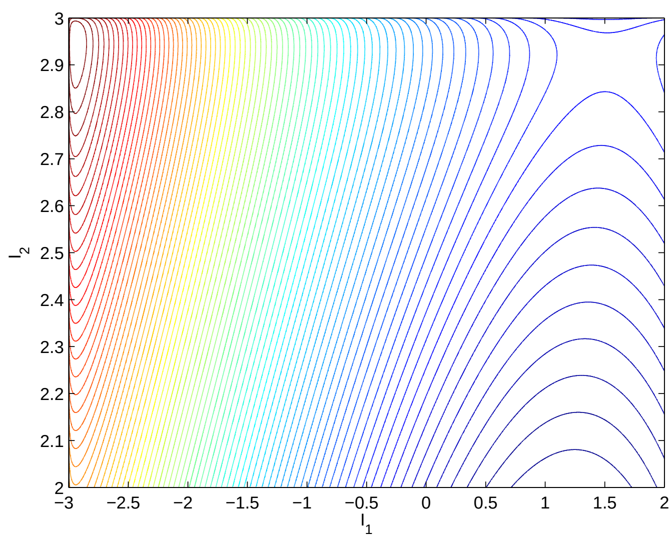

FIGURE 3. **Contours of $h(\theta_1, \theta_2)$, $\theta_1 = \theta_2 = 0$, in a subregion of the $(I_1, I_2)-$plane. $c = 3$, $\delta = -1.4$.**

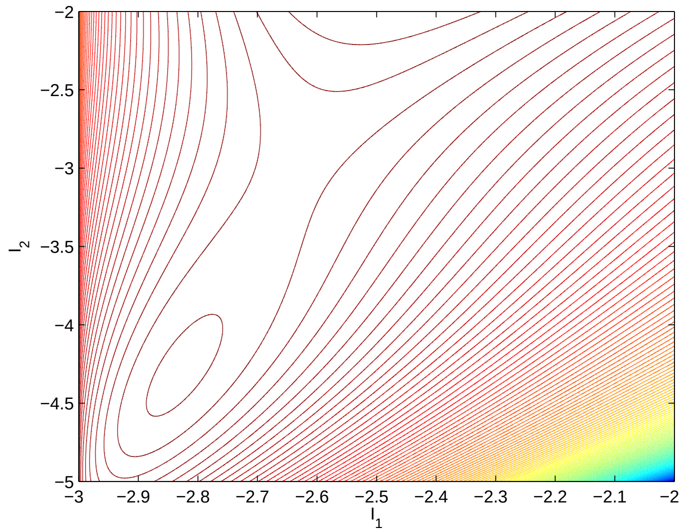

FIGURE 4. **Contours of $h(\theta_1, \theta_2)$, $\theta_1 = \theta_2 = 0$, in a subregion of the $(I_1, I_2)-$plane. $c = 3$, $\delta = -5.6$.**

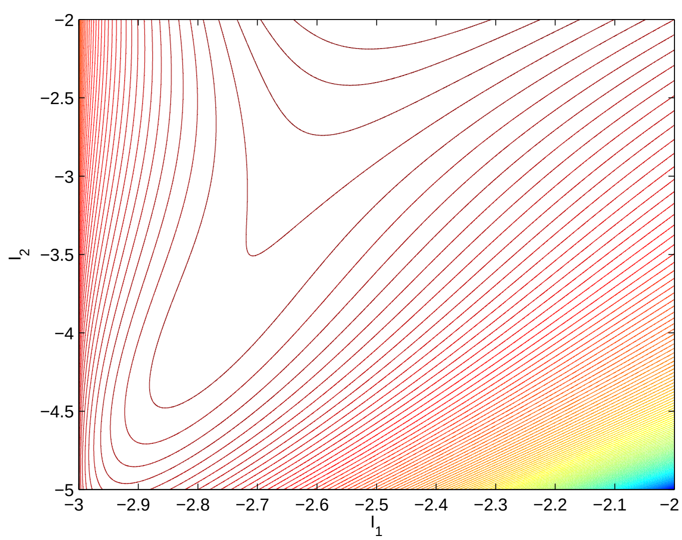

FIGURE 5. **Contours of $h(\theta_1, \theta_2)$, $\theta_1 = \theta_2 = 0$, in a subregion of the $(I_1, I_2)-$plane. $c = 3$, $\delta = -5.8$.**

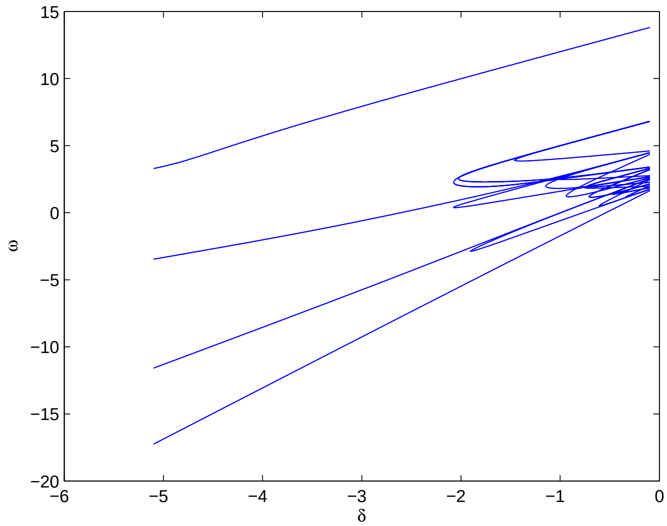

FIGURE 6. δ **vs.** ω **for all branches of symmetric breathers,** $N = 7$**,** $C = 7$**.**

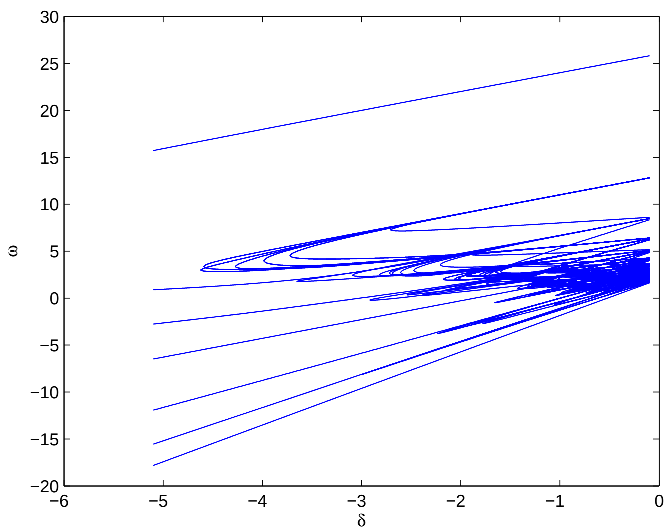

FIGURE 7. δ **vs.** ω **for all branches of symmetric breathers,** $N = 13$**,** $C = 13$**.**

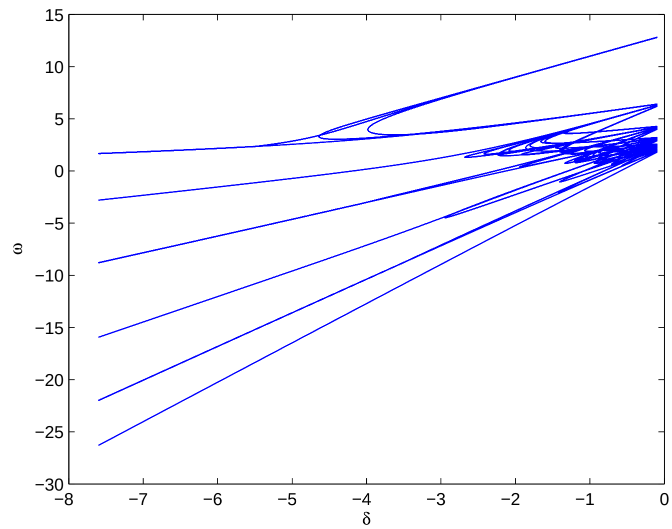

FIGURE 8. **δ vs. ω for all branches of antisymmetric breathers, $N = 13$, $C = 13$.**

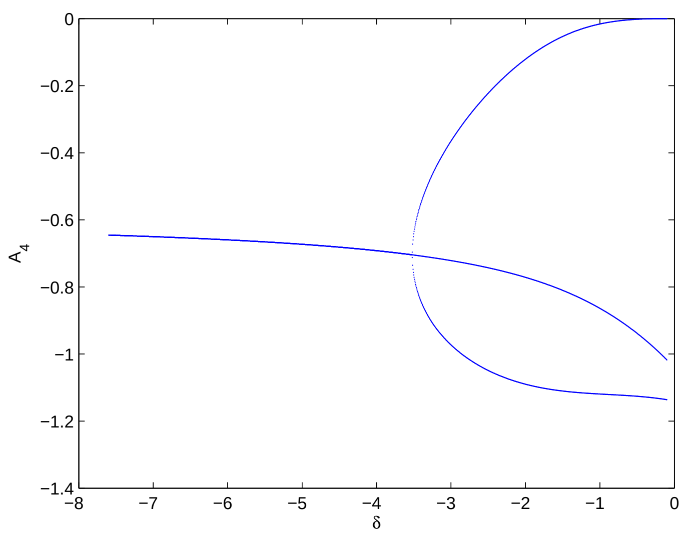

FIGURE 9. **δ vs. A_4 component of breathers continued from $\delta = 0$ antisymmetric breathers $[-1, 1, -1, -1, 1, -1, 0, \ldots]$ (middle), $[-1, 1, -1, 0, 1, -1, 0, \ldots]$ (top), $[-1, 1, 0, -1, 1, -1, 0, \ldots]$ (bottom). $N = 13$, $C = 13$.**

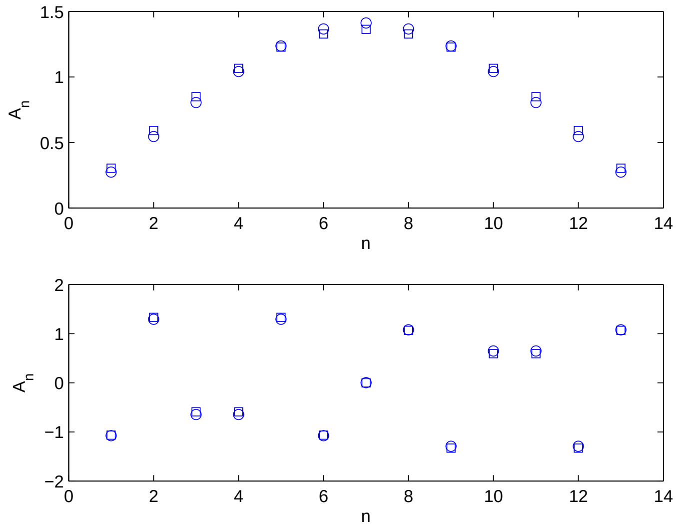

FIGURE 10. **(a) Continuation of $\delta = 0$ symmetric breather $[0,0,0,0,0,0,1,\ldots]$, $\delta = -75.0$ (square), linear normal mode (circle). (b) Continuation of $\delta = 0$ symmetric breather $[-1,1,-1,1,0,-1,1,\ldots]$, $\delta = -7.5$ (square), linear normal mode (circle).**

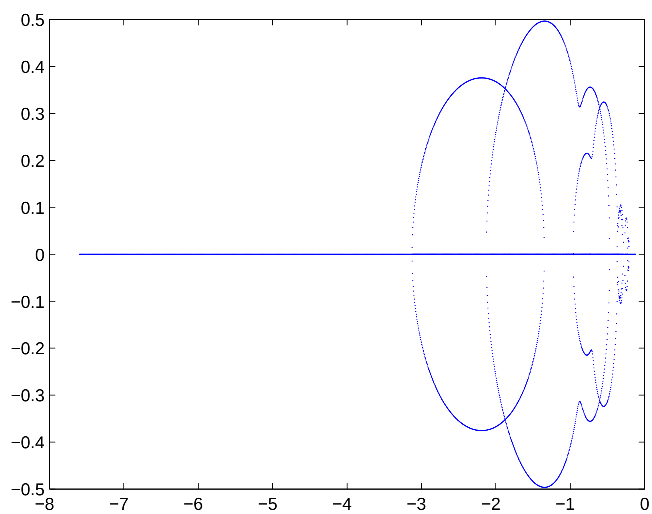

FIGURE 11. **$N013$, $C = 13$. δ vs. imaginary part of eigenvalues of $J\mathtt{H}$ for symmetric breather $[-1,1,-1,1,0,-1,1,\ldots]$.**